An optical levitation system for a physics teaching laboratory

Oscar Isaksson, Magnus Karlsteen, Mats Rostedt, and Dag Hanstorp

Citation: American Journal of Physics **86**, 135 (2018); doi: 10.1119/1.5007738
View online: https://doi.org/10.1119/1.5007738
View Table of Contents: https://aapt.scitation.org/toc/ajp/86/2
Published by the American Association of Physics Teachers

An optical levitation system for a physics teaching laboratory

Oscar Isaksson[a)]
Department of Physics, University of Gothenburg, SE-412 96 Gothenburg, Sweden and Department of Physics, Chalmers University of Technology, SE-412 96 Gothenburg, Sweden

Magnus Karlsteen
Department of Physics, Chalmers University of Technology, SE-412 96 Gothenburg, Sweden

Mats Rostedt and Dag Hanstorp
Department of Physics, University of Gothenburg, SE-412 96 Gothenburg, Sweden

(Received 23 December 2014; accepted 27 September 2017)

We describe an experimental system based on optical levitation of an oil droplet. When combined with an applied electric field and a source of ionizing radiation, the setup permits the investigation of physical phenomena such as radiation pressure, light diffraction, the motion of a charged particle in an oscillating electric field, and the interaction of ionizing radiation with matter. The trapping occurs by creating an equilibrium between a radiation pressure force and the force of gravity. We have found that an oil droplet can be trapped for at least nine hours. The system can be used to measure the size and total electric charge on the trapped droplet. The intensity of the light from the trapping laser that is scattered by the droplet is sufficient to allow the droplet to be easily seen with the naked eye, covered by laser alignment goggles. When oscillating under the influence of an ac electric field, the motion of the droplet can be described as that of a driven, damped harmonic oscillator. The magnitude and polarity of the charge can be altered by exposing the droplet to ionizing radiation from a low-activity radioactive source. Our goal was to design a hands-on setup that allows undergraduate and graduate students to observe and better understand fundamental physical processes.
https://doi.org/10.1119/1.5007738

I. INTRODUCTION

The use of a laser to move and trap macroscopic objects was first reported by Ashkin in 1970.[1] In the following year, an optical levitation trap was demonstrated by showing a glass bead being lifted and trapped by a single vertically aligned laser beam.[2] In an optical levitation setup, the radiation pressure from a laser beam counteracts gravity, producing a trap in the vertical direction, whereas the light refracted through the bead creates a force that restores the particle to the center of the beam in the horizontal plane. The loosely focused laser beam used in the experiment gives a large working distance, which means that the droplet is trapped far away from the focusing lens. A third optical trap invented by Ashkin is the optical tweezers.[3] This trap is created by directing a single laser beam down through a high-numerical-aperture microscope objective. One advantage of this trap is that a single microscope objective can be used for both trapping and observation; its main limitation is the short working distance. Since their invention in 1986, optical tweezers have played an important role in both research[4] and teaching. For example, a teaching application was demonstrated by Bechhoefer and Wilson, who described a low-cost experimental setup for optical tweezers to be used in undergraduate teaching laboratories.[5] Similarly, Appleyard *et al.*[6] introduced optical tweezers in teaching biology to undergraduate students. In an article by Smith,[7] it is shown how to build a tweezers setup for about $6500, and a full theoretical explanation of how the tweezers works was provided by Rocha.[8]

The other classical experiment of relevance to the present work is Millikan's oil drop experiment. In this experiment, a mist of small oil drops was produced in a cell in which a strong vertical static electric field was applied.[9] The free-fall velocity of the droplets was compared with their velocity when exposed to a vertical electric field. As a result, Millikan was able to cancel the effect of gravity and make a direct measurement of the charge on the droplets. Statistical analysis of the results of many measurements on different droplets allowed him to demonstrate the quantization of electric charge. Several versions of the Millikan experiment have subsequently been developed.[10,11]

A general trend in teaching experimental physics is the increased sophistication of the experimental tools, and this is particularly true in the case of quantum physics. For example, the introduction of relatively inexpensive computers, electronics, and improved detectors has made it possible to conduct experiments in high schools and colleges that, not too long ago, were only available in advanced research laboratories. Nuclear magnetic resonance, optical pumping, and superconductors are examples of such areas. However, many of these modern demonstration tools take the form of "black boxes," where the physics that goes on in the experiment are unseen. Of course, such tools allow students to perform beautiful experiments, but they grant limited insights into the methods of experimental physics. An example of such a black box is the small matchbox-sized USB-coupled spectrometers that are now commercially available.[12] These are perfect instruments for classroom demonstrations of phenomena such as atomic spectral lines, blackbody radiation, and the Fraunhofer lines of the solar spectrum. However, such experiments and devices do little to improve the experimental skills of students or their understanding of how spectrometers work. One interesting example in which an advanced experiment can be demonstrated without a sophisticated recording system is the Paul trap. In this "hands-on" setup, charged particles can be trapped using a combination of dc and ac electric fields.[13,14] Students can thus be introduced to a rather simple apparatus that is based on the same principles as used in investigations into atomic clocks, quantum computers, and antimatter. This connection to modern research makes it very attractive to students, while its simplicity makes it possible to demonstrate very fundamental physical phenomena in an easy way.

The objective of this paper is to describe an experimental system that we have developed to demonstrate advanced physics concepts. The system is a combination of optical manipulation and Millikan's experiment. The setup is relatively simple and uses basic instrumental tools found in reasonably well-equipped undergraduate laboratories. The experiment is built from standard components and can be easily modified by the student. The physics involves the trapping of charged droplets in a laser field, and the experiment can be used to demonstrate physical phenomena, such as radiation pressure, light diffraction, the movement of charged particles in electric fields, and ionization by radioactive sources. The system is open, and all these effects can be observed with the naked eye.

II. THE EXPERIMENTAL SETUP

A. Experimental procedure

Figure 1 shows a schematic view of the experimental setup. A vertically directed green ($\lambda = 532$ nm) laser beam is focused into the center of a rectangular cell. A plastic bottle with a volume of 1.5 l is placed upside-down straight above the cell. Oil droplets are sprayed into the bottle and allowed to descend downwards into the focal region of the laser beam, where they can become trapped just above the beam's focal plane. Once an oil drop has been trapped, the bottle is moved horizontally out of the laser beam.

A red laser beam ($\lambda = 633$ nm) is then directed horizontally onto the droplet, which creates a diffraction pattern that is used to measure the droplet's size. The vertical position of the droplet is measured by imaging the scattered light onto a position-sensitive detector (PSD). A vertically directed electric field is used to move the droplet up or down while still being trapped in the laser field. Finally, α-particles from a radioactive source can be introduced into the cell in order to alter the charge on the oil droplet.

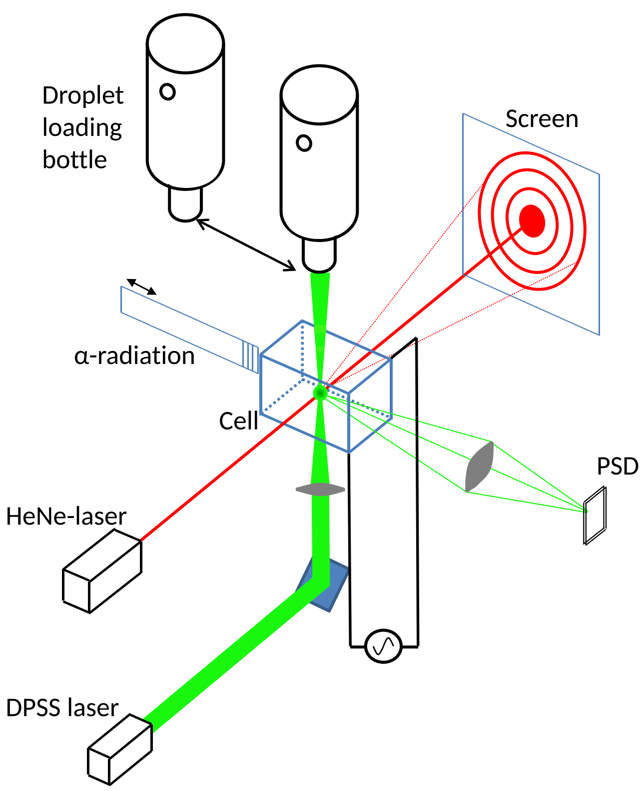

Fig. 1. Schematic view of the experimental setup. Two droplet-loading bottles are shown in the figure, in order to indicate the two positions of the bottle used in the experiment. See text for detailed discussion.

B. Technical description

Figure 2 shows a CAD representation[15] of the arrangement shown in Fig. 1. The experimental setup is placed on an optical table, although any stable table would suffice. The system is enclosed in light-absorbing boards (ThorLabs TB4) mounted on aluminum rails (ThorLabs XE25). For clarity, the two boards in the front have been removed from the drawing, and the two boards in the back have been made semi-transparent. A 60×45 cm breadboard (ThorLabs MB4560/M) is placed 150 mm above the level of the optical table using six pillar posts (ThorLabs RS6P4M). This forms the upper surface used for positioning the optical components.

The central part of the experiment is a rectangular cell $26 \times 36 \times 26$ mm in size. The top and bottom surfaces of the cell consist of two aluminum plates with 5-mm holes at their centers. The two plates are connected to a high-voltage power supply (± 1000 V), which is used to create a homogeneous vertically oriented electric field. Three of the side walls of the cell are made of microscope slide glass, and one side is made of acrylic glass with a 10 mm hole drilled in the middle. A polyethylene terephthalate (PET) bottle with a volume of 1.5 l is mounted upside-down on a vertical rod. A 10 mm hole has been drilled in the side of the bottle. Lubricating oil is sprayed from a can (CRC 5–56) into the 10 mm hole in the bottle. However, any system that can produce microscopic droplets can be used, such as the drop dispenser used for Millikan's oil drop experiments or spray nozzles for painting. The drop-loading bottle is mounted vertically above the trapping cell when it is used to trap a

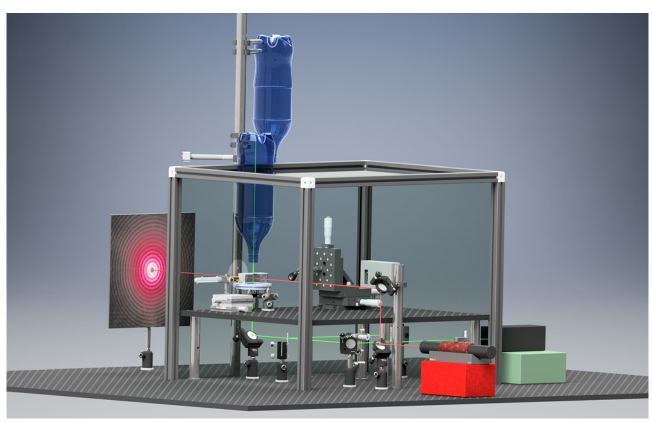

Fig. 2. A 3D CAD drawing showing the experimental setup. The system is enclosed in light-absorbing boards. For clarity, the two boards in front have been removed from the drawing and the two boards in back have been made semitransparent. A PDF version of the drawing is available as supplementary material (Ref. 15) and allows panning, rotating, and zooming; components can be removed one by one for clarity. The model numbers of all components used in the experiment are also presented in the PDF.

droplet. The bottle is rotated away from the cell as soon as a drop has been successfully trapped. In the CAD drawing, the two bottles illustrate these two positions.

The laser used for optical levitation is a 2 W diode pumped solid-state (DPSS) continuous-wave laser with a wavelength of 532 nm (Optlaser, China). This laser has an RMS stability of 5% and a divergence of 2.5 mrad and is placed outside the enclosure system. The laser light enters the enclosed system through an aperture in one of the absorbing boards. Two mirrors are mounted on precision mounts (Thorlabs KM100) to guide the laser light. The second mirror directs the laser beam upwards through a 10 mm hole drilled in the breadboard. The laser beam is focused using a 30 mm focal length lens mounted in a lens holder (Thorlabs LA1289 and SMR05/M). This lens is positioned so that the focal point falls in the center of the trapping cell. Unscattered laser light is collected using a beam block (Thorlabs LB1/M). A small fraction of the laser beam is split using a microscope cover glass and directed towards a photodetector (Thorlabs PDA36A-EC). This is used to continuously measure the relative laser intensity. This reading is calibrated by temporarily placing a laser power meter in the trapping cell's position.

The setup also contains optical components for measuring the size and position of the droplet. Its size is determined from the diffraction pattern produced on a screen 25 cm from the droplet by a red beam ($\lambda = 633$ nm) from a 4 mW HeNe laser (Uniphase 1101P), which is directed onto the droplet using two mirrors.

The position of the droplet is measured using a PSD (Sitek Electro Optics AB S1–0006). Light scattered from the droplet is collected by a 21 mm positive lens and focused on the PSD. The PSD is a 20 mm-long resistive photodiode. The electric current created by the light is collected from the two ends of the diode. The vertical position y of the light hitting the diode can be calculated using the expression

$$y = \frac{L}{2}\left(\frac{I_1 - I_2}{I_1 + I_2}\right), \tag{1}$$

where L is the length of the PSD and I_1 and I_2 are the output currents from the ends of the PSD. The measurement of position y by the PSD is used to adjust the laser power, in order to keep the droplet levitated at a constant height. This procedure is performed by a LABVIEW program, in which a set-point for the position is defined. The height of the droplet can be kept at the set-point by tracking its position while continuously adjusting the laser power.

Finally, a radioactive source is mounted on a XYZ translation stage (Thorlabs XR25C) to the left of the cell. This radioactive source is an α-emitter (^{241}Am, 5.5 MeV) with an activity of 37 kBq. The source is aimed towards the droplet through a 10 mm hole in the acrylic glass. In order to reduce the flux of alpha particles, the hole is covered with perforated tape.

C. Safety

The trapping laser, the high-voltage supply, and the radioactive source are all potentially harmful. Safety precautions aimed at preventing any incidents are very important and are discussed in this section.

The DPSS laser used for trapping is a 2 W cw laser, with a power of 0.9 W being used in the experiment. Since the laser can damage eyes, laser goggles must be used in the laboratory. We use alignment goggles (Phillips Safety Products model LS-AA-33-BK), which transmit only a small fraction of the light at 532 nm. It is thus possible to align the system while wearing the goggles. As an extra precaution, the experimental setup is also enclosed by light-absorbing boards, as described in Sec. II B, which reduces the scattered light in the laboratory. The unscattered light from the laser is collected using a beam block. To work in the laboratory, all students must learn laser safety procedures.

A high-voltage power supply is employed to create the electric field that moves the electrically charged droplets. The electrodes are carefully enclosed to avoid any contact with users. The voltage supply is only used to place the plates in the cell at an electric potential; no current is drawn through system. Potential hazards are minimized by using a power supply that cannot deliver more than 0.1 mA. Alternatively, a large resistance ($R > 10$ MΩ) can be placed between the output of the power supply and the plates in the cell.

The radioactive source used in the experiment is approved for educational use by the Swedish Radiation Safety Authority. Its activity is less than 50 kBq, and it is mounted in a holder to prevent direct contact with the source.

III. EXPERIMENTS

A. Radiation pressure

The main objective of this work is to introduce an experimental setup that is capable of investigating the physical process of optical levitation. This is a process in which radiation pressure, a result of photons carrying momentum, is used to trap microscopic particles in air. The concept of radiation pressure was first mentioned by Kepler in 1619 as a way of explaining why the tail of a comet always is directed away from the sun. Maxwell showed theoretically that an electromagnetic field exerts a force on a material object, and this prediction was experimentally verified by Lebedev[16] in 1901 and by Hull and Nichols in 1903.[17]

In the quantum physics picture, the momentum of light depends on frequency according to

$$p = \frac{h}{\lambda} = \frac{h\nu}{c}, \tag{2}$$

where h is Planck's constant, λ is the wavelength of light, ν is the frequency, and c is the speed of light. Thus, as a consequence of the conservation of momentum, there will be a change in the momentum of a particle from which light is scattered. The resulting radiation pressure force on the particle, $F_{\rm rad}$, can be expressed as[18]

$$F_{\rm rad} = Q_r \frac{P}{c}, \tag{3}$$

where P represents the laser power directed at the particle, c is the speed of light, and Q_r is a dimensionless factor. The quantity $Q_r = 1$ if all the light is absorbed by the particle, $Q_r = 0$ if all the light is transmitted by the droplet, and $Q_r = 2$ if all the light is reflected back by the particle.

In the experimental setup for optical levitation, droplets are created by spraying lubrication oil into the droplet-loading bottle (Fig. 1). Droplets descend down the laser beam through a small aperture in the top plate of the experimental cell. The radiation pressure increases as the droplet descends towards the laser focus, and at some point, the radiation pressure will balance the gravitational force. This situation is shown in Fig. 3(a). Droplets will be trapped slightly above the focal plane of the laser beam. Ray-tracing simulations show that droplets with a radius on the order of $10\,\mu$m will be stably trapped 1 mm above the focal plane when a laser power of 0.9 W is used.

Trapping in the horizontal plane is caused by light being refracted by the droplet. Figure 3(b) shows a droplet displaced from the center of the laser beam in the horizontal plane. In this figure, $R1$ and $R2$ represent the strong and weak fraction of the laser beam refracted by the droplet, which causes the recoil forces on the droplet marked $F1$ and $F2$. Because $F1$ is larger than $F2$, the result is a net force towards the more intense part of the beam. The droplet will hence move sideways until it is centered on the laser beam. In this way, the droplet also becomes trapped in the horizontal plane.

A photograph of a trapped droplet is shown in Fig. 4. The droplet is scattering intense green light and is easily observed by the naked eye when the laser alignment goggles are used. Droplets descend down through the cell with one of them becoming trapped in the laser beam. The longest trapping time we have observed so far is nine hours, at which point the laser was switched off, ending the trap. The experiment clearly demonstrates how radiation pressure associated with laser light is sufficiently strong to balance the gravitational force. The radiation pressure can be further demonstrated by observing how the drop can be moved in the vertical direction by changing the intensity of the laser.

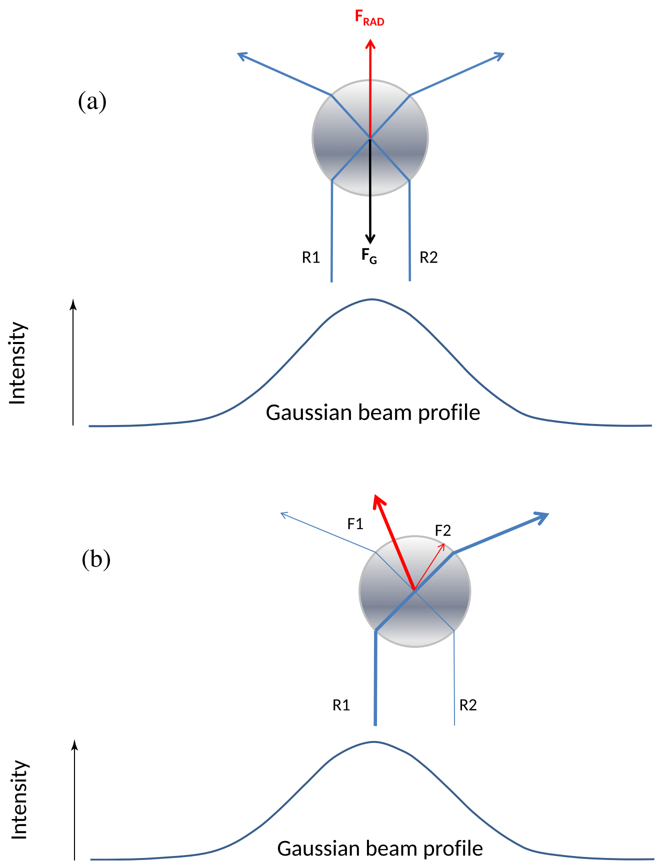

Fig. 3. (a) The position of the droplet in the focused laser beam where the photon pressure and the gravitation force balance each other out. (b) The droplet displaced from the center of the laser beam in the horizontal plane. $F1$ and $F2$ are the recoils caused by the beams $R1$ and $R2$. The droplet will move sideways until it is centered in the laser beam. This demonstrates how the droplet is trapped in the horizontal plane.

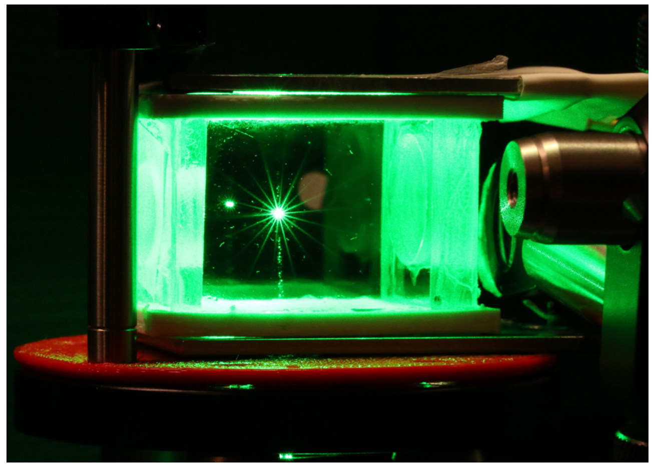

Fig. 4. A picture of a trapped droplet. Intense green light is scattered in all directions from the droplet.

B. Diffraction

The sizes of the droplets can be determined using two different methods. The first method, described here, is to analyze the diffraction pattern produced when laser light is shone on the droplets. The second method will be discussed in Sec. III F. The theory of diffraction can be found in standard optics textbooks.[19] For a circular object illuminated by laser light, the irradiance on a screen set at a large distance from the scattering region is given by

$$I(q) = I(0)\left[\frac{2J_1(kaq/R)}{kaq/R}\right]^2, \tag{4}$$

where $I(0)$ is the maximum irradiance in the center of the screen, $k = 2\pi/\lambda$ is the wavenumber, a is the radius of the object, q is the radial distance from the center of the diffraction pattern, $J_1(x)$ is the Bessel function of the first kind, and R is the distance between the object and the screen. The condition for “large distance” is given by

$$\frac{a^2}{R\lambda} \ll 1, \tag{5}$$

a condition that is met in this experimental arrangement. The first dark ring corresponds to the first minimum of the Bessel function. A measurement of the quantities q and R allows us to determine the radius of a droplet using

$$2a = 1.22\frac{R\lambda}{q}, \tag{6}$$

where a is the radius of the droplet. In our experiment, the trapped droplet is irradiated with a horizontally directed beam from a 4 mW HeNe laser to create the far-field diffraction pattern, as shown in Fig. 5(a).

There is a relatively large distribution in the size of the droplets produced from the spray can, and the probability that a droplet will be trapped depends on its size. A convolution of these two functions of the droplet size can be investigated by measuring the size distribution of a sequence of trapped droplets. This is shown in Fig. 5(b). Only droplets that were stably trapped for at least one minute were included in the dataset. The graph shows that droplets with

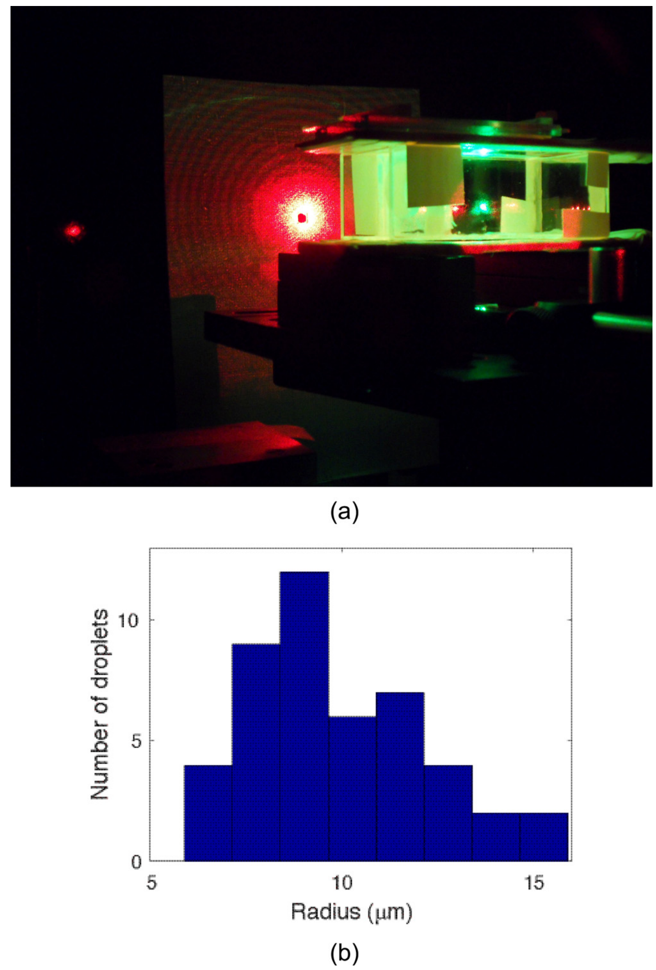

Fig. 5. (Top) Diffraction pattern created by a trapped droplet. The dark spot in the center of the diffraction pattern is a hole made to allow unscattered light through. (Bottom) Size distribution of a sequence of trapped droplets. The droplets were trapped with a laser power of 900 mW.

radii between 6 ± 0.9 and $16 \pm 0.9\,\mu$m are trapped in this experiment. This uncertainty is associated with the measurement of q, the radial distance from the center to the first minimum in the diffraction pattern. The range of radii, combined with the known density of the oil (0.81 g/cm^3), yields a range in droplet weights of 7×10^{-12} to 1.4×10^{-10} N. This experiment clearly visualizes the wave nature of light, demonstrating that micrometer-size droplets scatter light to produce a far-field diffraction pattern that can be measured using a simple millimeter-scaled ruler.

C. Optical imaging and droplet motion

The motion of the droplets is measured by imaging the scattered green trapping light either onto a PSD or onto a screen, using a lens with a focal length of $f = 21$ mm. The position of the lens needed for a sharp image is given by the thin lens formula

$$\frac{1}{f} = \frac{1}{a} + \frac{1}{b}, \tag{7}$$

where a is the distance from the droplet to the lens and b is the distance from the lens to the image. The magnification (M) of the movement of the drop is given by

$$M = -\frac{b}{a}. \tag{8}$$

In our system, we have $a = 2.6$ cm and $b = 13$ cm, giving a particle motion magnification of $M = 5$ when the lens is positioned to produce a sharp image on the PSD. By choosing these distances, vertical movements of the droplet of up to 4 mm can be registered by the 20 mm long PSD. Alternatively, by setting a to be just over 2.1 cm and $b = 200$ cm, a magnification of almost 100 is obtained. The motion of the droplets can then clearly be observed on a screen, making it possible to measure the varying position of the droplet using a millimeter-scaled ruler.

D. The motion of charged particles in electric fields

Droplets generally become electrically charged when they are sprayed from nozzles; both positively and negatively charged droplets are observed. The charge makes it possible to displace a trapped droplet vertically using an applied electric field. The direction of the motion then depends on the sign of the droplet's charge and on the polarity of the electric field. We can apply dc electric fields, which displace the droplet, and ac electric fields, to make the droplet oscillate around its equilibrium position. Electric fields of up to 400 V/cm can be applied across the cell. Figure 6 shows the position of the droplet as measured by the PSD when an ac electric field has been applied.

The motion observed in the figure is almost in phase with the electric field, indicating that the charge on the droplet is positive. The droplet reaches its peak displacement slightly after the electric field reaches its maximum value. This phase lag is due to air resistance in the cell, as will be further discussed in Sec. III F. The friction is sufficiently large to make the system overdamped. Negatively charged droplets will oscillate out of phase with respect to the applied electric field, but the small phase lag due to the friction in air will of course also occur for negatively charge droplets.

E. Absolute measurements of the electrical charge

The absolute value of the charge of a droplet can be determined using the method first suggested by Ashkin and Dziedzic[20] in 1975. First, a droplet is trapped in the laser beam and its size is measured as described in Sec. III B, or the size is calculated using the phase difference (to be discussed in Sec. III F). The mass of the droplet and hence the

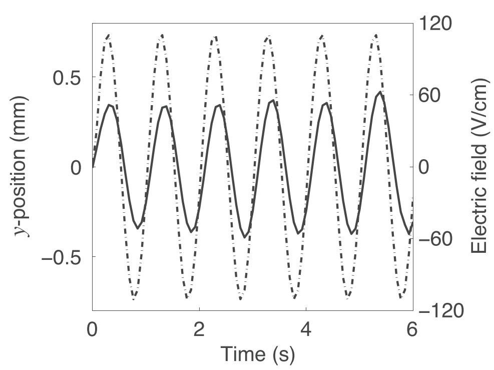

Fig. 6. The relative motion of a droplet exposed to an ac electric field. The dashed line displays the electric field (scale to the right), while the solid line shows the relative y-position measured with the PSD (scale to the left).

gravitational force F_{mg} acting on it can then be determined. The droplet is trapped at the position where the radiation force F_{rad1} balances gravity, i.e., when

$$F_{mg} = F_{\mathrm{rad1}}. \tag{9}$$

This situation is shown on the left in Fig. 7. Thereafter, the droplet is moved upwards by applying a vertically oriented dc electric field. This situation is shown in the middle of Fig. 7. The droplet now experiences an additional electric force F_E in the upward direction. Finally, the trapping laser power is decreased until the droplet returns to its original position. This situation is shown on the right of Fig. 7. The gravitational force is now balanced by the sum of the forces from the radiation pressure F_{rad2} and the force from the electric field F_E, according to the expression

$$F_{mg} = F_{\mathrm{rad2}} + F_E. \tag{10}$$

At this point, the drop experiences a laser field with the same geometrical profile, but with a lower intensity, as shown on the left side of Fig. 7. By combining Eqs. (9) and (10), we obtain

$$F_E = \left(\frac{F_{\mathrm{rad1}} - F_{\mathrm{rad2}}}{F_{\mathrm{rad1}}}\right) F_{mg}. \tag{11}$$

Hence, the force from the electric field on the droplet F_E can be calculated using the known relative change in the laser power. The absolute charge on the droplet Q is then simply the ratio of the electric force on the droplet arising from the corresponding field strength E. The latter quantity can be calculated from the separation of the aluminum plates d and the applied voltage U. The absolute charge on the droplet will then be given by

$$Q = \frac{F_E}{E} = \frac{F_E d}{U}. \tag{12}$$

In Fig. 8, we plot the strength of the applied electric field (top), the vertical position of the droplet position (middle), and the laser power (bottom) as a function of time. The experimental data are recorded using a LABVIEW program. In this experiment, a feedback loop was used to regulate the laser power in order to keep the droplet in the same y-position ($y = 0$). However, it is also possible to perform the experiment by manually regulating the laser power. The double peak structure in the measurement of the positions, which occurs when the electric field is changed, is caused by slightly too large feedback parameters in the regulating system.

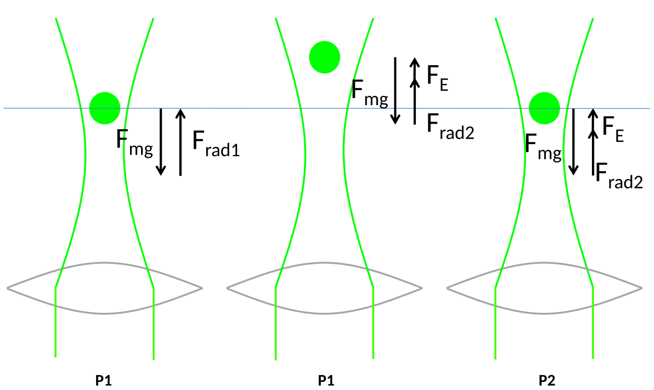

Fig. 7. A schematic sketch showing the procedure for measuring the absolute charge of a droplet, as described in the main text.

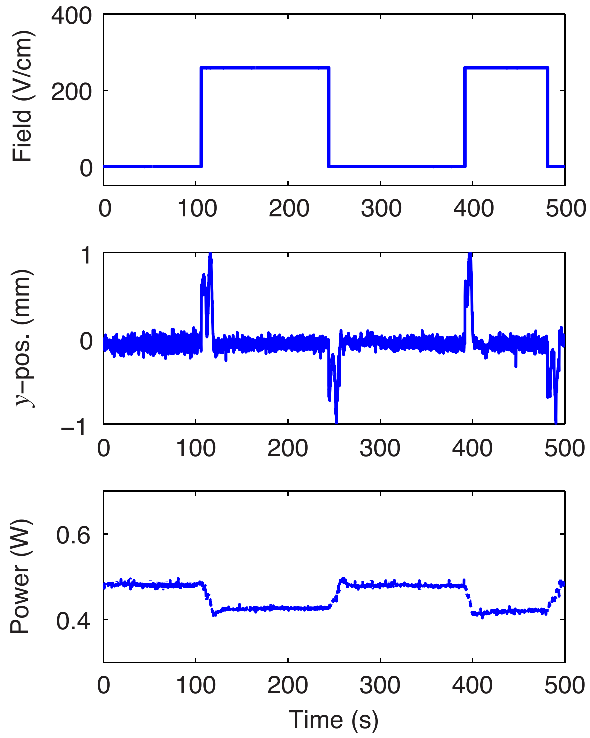

Fig. 8. The electric field applied over the cell (top); the relative y-position of the droplet (middle); the laser power applied to keep the droplet at $y = 0$ mm (bottom).

The measured charge of different trapped droplets varies considerably. In some cases, the drops are uncharged. The maximum charge we have observed is 8.9×10^{-17} C. When the total charge on the droplet is known, the excess or deficiency of electrons can be calculated. For example, 8.9×10^{-17} C corresponds to 550 excess electrons. The case shown in Fig. 8 corresponds to a droplet with about 70 excess electrons. The uncertainty in the charge determination is ± 3 elementary charges.

F. A damped driven harmonic oscillator

As shown in Sec. III D, the droplet can be moved up or down by applying a vertical electric field. A phase difference between the driving ac field and the position of the droplet is then observed. This phase difference can be used as a second method to determine the size of the trapped droplet.

When a vertical ac field is applied across the cell, the droplet begins to oscillate around the trapping position. It behaves like a driven damped harmonic oscillator with a spring constant k, a damping force b, and a driving force of $F_{\mathrm{el}} = Eq \sin(\omega t)$ from the electric field. The equation of motion for the oil droplet is given by[21]

$$\frac{d^2 y}{dt^2} + \gamma \frac{dy}{dt} + \omega_0^2 y = \frac{Eq}{m} \sin(\omega t), \tag{13}$$

where y is the vertical displacement, $\omega_0 = \sqrt{k/m}$, $\gamma = b/m$, and ω is the angular frequency of the driving field. The solution to this inhomogeneous differential equation is expressed as

$$y = A(\omega)\sin(\omega t - \alpha), \tag{14}$$

where α is the phase difference between the driving field, and the position of the oscillating object is given by

$$\alpha = \frac{\pi}{2} + \arctan\left(\frac{\omega^2 - \omega_0^2}{\gamma\omega}\right) = \frac{\pi}{2} + \arctan\left(\frac{m2\pi}{Tb} - \frac{kT}{2\pi b}\right). \tag{15}$$

Here, m, b, and k are the parameters that depend on the oil drop radius, and T is the period of the oscillatory motion. The damping is due to friction from air, the strength of which depends on the radius of the droplet. If the pressure in the cell were lower, the phase difference would be smaller and would change sign as the frequency reaches the resonance frequency. The spring constant k is calculated using F_E from Eq. (11) divided by the displacement, giving

$$k = \frac{0.035mg}{\Delta y}. \tag{16}$$

The phase shift α can be determined experimentally, and this value can then be used to determine the size of the droplet. In Fig. 6, the phase shift is $\alpha = 0.50$ rad, giving the equation

$$\frac{r^3(16\pi^3)\rho}{3} - 12r\pi^2\eta T\tan\left(\alpha - \frac{\pi}{2}\right) - \frac{0.035\,(4\pi r^3)\,9.82\rho}{3(25\times 10^{-6})}T^2 = 0. \tag{17}$$

For $\rho = 810\,\mathrm{kg/m^3}$, $\eta = 16.7\times 10^{-6}$ N s/m^2, and $T = 1$ s, the equation has one physically relevant solution, giving $r = 9.0\,\mu$m. The dominating error is in the determination of Δy; this originates from the uncertainty in the magnification of the movements by the lens on the PSD, with a value of $\pm 0.6\,\mu$m. Hence, this experiment gives the radius of the droplet as $r = 9.0 \pm 0.6\,\mu$m. The size of the same droplet determined using the diffraction pattern, as described in Sec. III B, yielded a value of the radius of $9.8 \pm 0.9\,\mu$m.

G. Interaction between matter and ionizing radiation

We now wish to investigate how the amplitude of oscillation of the droplet in an ac electric field varies as the charge on the droplet is changed. The charge on the droplet can be altered by exposing it to ionizing radiation. For this, we use a ^{241}Am radioactive source that emits α-particles with an energy of 5.5 MeV and a half-life of 432.2 years. According to Cooper and Reist,[22] the distance that α-particles with an energy range of $4 < E < 8$ MeV travel in air can be estimated by the equation $R_\alpha = 1.24E - 2.62$, where R_α is the distance in cm and E is the energy in MeV. In the present experiment, the α-source is placed about 2 cm from the droplet, so according to this equation the α-particles travel about 4.2 cm in air.

The positively charged α-particle loses kinetic energy via the Coulomb interaction in collisions with atomic electrons in the air. The energy needed to ionize air is around 34 eV, indicating that about 160 000 positive ions and electrons can be released by a 5.5 MeV α-particle. The released electrons or positive ions can subsequently attach, through electromagnetic interaction, to the droplet, thus increasing or decreasing the charge on the droplet. Ionizing events might also appear inside or on the surface of the droplet. Other types of ionizing radiation, such as β and γ radiation, would also produce the same charge-changing effect on the droplet, though with a smaller cross-section.[23] Figure 9 shows how the amplitude of the oscillations decreases in the presence of the ^{241}Am source. The initial number of excess electrons in the data given in Fig. 9 is about 40. By observing the temporal change in the oscillation amplitude, we estimate that 2–3 electrons are removed from the droplet per second. It is likely that each α-particle removes more than one electron from the droplet.

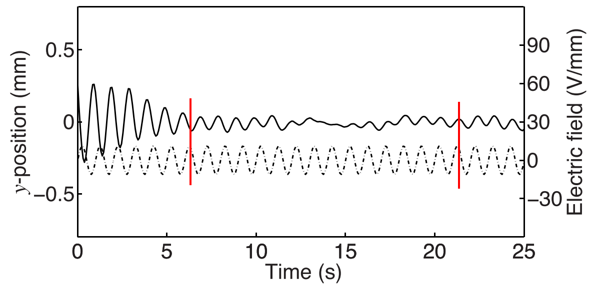

Fig. 9. Phase shift of the oscillations. The solid curve represents the position and the dotted curve the electric field. At the first vertical line, the droplet is out of phase with the electric field; at the second vertical line, the position and the field are in phase. This phase change demonstrates that the polarity of the droplet has been changed.

Also, note that before $t = 10$ s, the droplet is oscillating almost 180° out of phase with the electric field, and after $t = 20$ s, it is almost in phase with the field. All other experimental parameters have been kept constant. This observation must thus be due to the droplet changing from having a negative charge to having a positive charge.

IV. DISCUSSION

The experimental system presented in this paper is designed to be used as an instructional tool at different levels of education. We have already used it in various educational environments. For example, demonstrations have been made for smaller groups in the laboratory and with larger groups with the help of web cameras. In such demonstrations, we show, for example, how the force associated with radiation pressure can counteract gravity, how a diffraction pattern can be used to determine the size of a droplet, and how charged droplets behave in an applied electric field. In an undergraduate laboratory, the students are able to first trap a droplet and then measure the size and charge on the droplet in a half-day laboratory exercise. In this environment, the student begins the exercise with all the optics mounted and aligned. The goal is to use the setup to perform the experiments that are described in Sec. III.

At a more advanced level, which might meet the requirements for an experimental project in a bachelor's degree, students are required to build their own system, beginning from an empty optical table. Having performed the above measurements, they are requested to investigate the feasibility of other possible measurements. The system is very suitable for open-ended projects where the students can, for instance, investigate the size or charge distribution of droplets, the evaporation rate of a droplet, or the trapping probability. As an example, one group of bachelor's students investigated trapping multiple drops by keeping the droplet-loading bottle in place after the first drop had been trapped. They observed both the trapping of multiple drops and the coalescence of droplets by filming the process with a simple web camera.

V. CONCLUSION AND OUTLOOK

In this paper, we have presented an experimental system that involves the optical trapping of an oil droplet. The setup is easy to operate and the outcome is quite spectacular to observe. It certainly captures the attention of students. The size of the droplets can be determined by either analyzing a diffraction pattern or studying their damped motion in an oscillating electric field. The results obtained by the two methods are in agreement within their uncertainties. The setup can also be used to determine the electric charge on the levitated droplet and to change this charge *in situ* using ionizing radiation. The arrangement is such that students can make hands-on measurements and thus gain valuable experience in practical experimental physics. The setup has been tested with both undergraduate and graduate level students, with positive results. The system is flexible, making it suitable for open-ended experiments on an advanced level.

In this experiment, we have described how to make an absolute measurement of the total charge on a droplet with an uncertainty of ± 3 elementary charges. By reducing the uncertainty, it should be possible to observe quantization of the charge. The resolution is limited in precision by Brownian motion, which will produce random changes in the position of the droplet, electronic noise in the PSD detector, and noise in the feedback loop between the PSD detector and the laser power supply. The Brownian motion could be reduced by evacuating the interior of the cell in which the droplet is levitated, and the noise in the detection system could be reduced by modulating the trapping laser with a high frequency and using a lock-in detection scheme. (The probability ionizing the droplet with the radiation will then be reduced, but this can be compensated for by placing the radiation source closer to the droplet.) With these improvements, we should be able to observe plateaus in the amplitude that correspond to integer numbers of excess electrons on the droplet. Such a measurement requires that the excess electrons are emitted one at a time. This, in turn, might require that the α-source used to remove excess electrons is replaced with a UV light source.

ACKNOWLEDGMENTS

This work was supported by the Swedish Research Council. O.I. gratefully acknowledges Sannarpsgymnasiet, Halmstad for their support. Thanks to Ivan Galinskiy for his valuable support, both in the laboratory and with the manuscript. David Pegg, Remigio Cabrera-Trujillo, Göran Nyman, and Jonas Enger are acknowledged for valuable input on the manuscript.

[a]Electronic mail: oscar.isaksson@physics.gu.se

[1]A. Ashkin, Phys. Rev. Lett. **24**, 156–159 (1970).
[2]A. Ashkin and J. M. Dziedzic, Appl. Phys. Lett. **19**, 283–285 (1971).
[3]A. Ashkin, J. M. Dziedzic, J. E. Bjorkholm, and S. Chu, Opt. Lett. **11**, 288–290 (1986).
[4]J. P. Reid, J. Quant. Spectros. Radiative Transfer **110**, 1293–1306 (2009).
[5]J. Bechhoefer and S. Wilson, Am. J. Phys. **70**, 393–400 (2002).
[6]D. C. Appleyard, K. Y. Vandermeulen, H. Lee, and M. J. Lang, Am. J. Phys. **75**, 5–14 (2007).
[7]S. P. Smith, Am. J. Phys. **67**, 26–35 (1999).
[8]M. S. Rocha, Am. J. Phys. **77**, 704–712 (2009).
[9]R. A. Millikan., Phys. Rev. **2**, 109–143 (1913).
[10]R. C. Jones, Am. J. Phys. **63**, 970–977 (1995).
[11]K. J. Silva and J. C. Mahendra, Am. J. Phys. **73**, 789–797 (2005).
[12]USB4000, 2015.
[13]H. Winter and H. W. Ortjohann, Am. J. Phys. **59**, 807–813 (1991).
[14]A. Schmitt, N. Coberger, and K. Wendt, PdN Phys. Sch. **59**, 3–8 (2010).
[15]See supplementary material at http://dx.doi.org/10.1119/1.5007738 for CAD drawings. For more information see <https://chalmersuniversity.box.com/v/OpticalLevitationSetup>.
[16]P. Lebedev, Ann. Phys. **6**, 1–26 (1901).
[17]E. F. Nichols and G. F. Hull, Phys. Rev. **17**, 26–40 (1903).
[18]A. Ashkin, Biophys. J. **61**, 569–582 (1992).
[19]E. Hecht, *Optics*, 3rd ed. (Freeport, New York, 1998).
[20]A. Ashkin and J. M. Dziedzic, Science **187**, 1073–1075 (1975).
[21]D. C. Giancoli, *Physics for Scientists and Engineers*, 4th ed. (Upper Saddle River, New Jersey, 2008).
[22]D. W. Cooper and P. C. Reist, J. Colloid Interface Sci. **45**, 17–26 (1973).
[23]W. R. Leo, *Techniques for Nuclear and Particle Physics Experiments. A How-to Approach*, 1st ed. (Springer-Verlag, Berlin- Heidelberg, 1994).